426. Simulation of sticking of adhesive particles under normal impact

R. Jasevičius[1,a], R. Kačianauskas[1,b], Jürgen Tomas[2,c]
[1]Vilnius Gediminas Technical University, Lithuania,
[2]Otto-von-Guericke Magdeburg University, Germany
e-mail: [a]*raimondas.jasevicius@fm.vgtu.lt*, [b]*rimantas.kacianauskas@fm.vgtu.lt*,
[c]*juergen.tomas@ovgu.de*

(Received 12 January 2009; accepted 10 March 2009)

Abstract. Sticking of adhesive spherical particles under normal impact is investigated numerically by applying the Discrete Element Method. The nonlinear-dissipative contact model with adhesion is applied to model normal contact forces. Loading is described by elastic Hertz and elastic-plastic contact model with history-dependent adhesion. Damping is described by nonlinear Tsuji model. Adhesion limit is of linear character while particle detachment is of non-linear nature. Sticking and detachment behaviour for various damping values are considered in detail. Influence of the adhesion force for a wide range of particle sizes is illustrated by the variation of critical sticking velocity. Comparison of purely elastic with elastic-plastic behaviour is also presented.

Key words: cohesive granular material, normal elastic-plastic contact, sticking and detachment, critical sticking velocity, discrete element method

Introduction

The handling of granular materials is of great importance in pharmaceutical, food, cement, chemical and other industries. The problems relevant to particle segregation, the effects of granular material vibration, attrition, breakage, dust explosions and other phenomena have been encountered during the operation period of many processing apparatuses and machines. The granular state of the material is a transient state between gas, liquid or solid [1, 2], implying that the material possesses some of their properties and behaves either similarly or in a completely different manner.

Historically, a major part of granular materials has been treated as an assembly of non-adhesive grains or particles. The rapidly increasing production of poly-dispersed dry cohesive powders causes much more serious technical problems associated with undesired adhesion in particle conversion or powder handling, and desired adhesion in agglomeration or coating. Thus, understanding the fundamentals of particle adhesion with respect to product quality assessment and process performance is highly needed in powder technology.

Cohesive granular materials are currently being studied by applying experimental, theoretical and numerical methods. Recently, the discrete (distinct) element method (DEM) introduced by Cundall and Strack [3] has become a powerful tool for solving many scientific and engineering powder technology problems. It was first applied to simulate the dynamic behaviour of non-cohesive granular material, which is presented as an assembly of particles. Interaction of particles described by the Hertz contact theory is usually used to describe repulsive contact forces not depending on the specific particle size. Fundamentals of the DEM and particular

models of non-cohesive granular material may be found in [4-7], while the important details of simulation technique and software implementation are presented in [8-11].

Investigation of the nature of adhesive particles required the application of new models. Independently of the development of the discrete element method, an expression of the normal force for spherical particles was suggested by Johnson, Kendall and Roberts [12]. This JKR model assumes that the surface attraction force only results in the change in surface energy within the contact area. Derjaguin, Muller and Toporov et al. [13] considered that the surface attraction forces have a finite range and, therefore, act just inside and outside the contact zone where surface separation is small. This model is known as DMT model. The first comprehensive physical models for fine particles were described by Molerus [14, 15]. The earliest discussions about the simplest adhesion (surface attraction) models and the importance of these effects for the results of simulation of granular material behaviour were presented by Thornton and Yin [16] and Kohring [17]. Comprehensive research on cohesive powders was continued by Tomas [18-20]. Fundamentals of cohesive powder consolidation and flow are generalized in [20]. In this work, the model of "stiff particles with soft contacts" was used for ultrafine particles (with the diameter $d < 10$ μm). This hysteretic model describes the elastic-plastic particle contact behaviour with adhesion and hysteretic load-unload-reload. Some other interesting contributions and DEM simulations may be also mentioned. For example, shear behaviour of cohesive powders with friction was studied by Luding [21, 22] and Tykhoniuk et al. [23]. Cohesive powders combining contact elasticity and distant van der Waals-type attraction were simulated by Gilabert et al. [24]. Collision dynamics of granular particles with visco-elastic adhesion was considered by Brilliantov et al. [25]. The authors focused basically on characterizing restitutive collisions described by the coefficient of restitution as well as sticking in collisions described by the critical sticking velocity. Elastic-plastic adhesion of ultrafine powders was considered by Tomas [26-27]. The paper addresses simulation of sticking of adhesive particles under normal impact. The non-elastic Hertz and elastic-plastic contact models with linear adhesion in contact compression and Tsuji damping are applied to model normal contact forces. Sticking and detachment behaviour is illustrated in details. The influence of the adhesion force is illustrated by varying critical sticking velocity for a wide range of particles with respect to their size.

Simulation methodology

In the present work, the DEM methodology based on the Langrangian approach is applied to simulate the dynamic behaviour of the adhesive particles under normal impact. From the perspective of modeling, smooth spherical particles considered may be termed discrete elements. When moving, the particles impact and deform each other.

The motion of arbitrary particle i is characterized by a small number of global parameters, e.g. positions $\mathbf{x}_i$, velocities $\dot{\mathbf{x}}_i = \mathrm{d}\mathbf{x}_i / \mathrm{d}t$ and accelerations $\ddot{\mathbf{x}}_i = \mathrm{d}^2\mathbf{x}_i / \mathrm{d}t^2$ of the mass center and a force applied to it. Translational motion is described by the Newton's second law applied to each particle i as follows:

$$m_i \ddot{\mathbf{x}}_i(t) = \boldsymbol{F}_i(t), \qquad (1)$$

where m_i is the mass, while vector $\boldsymbol{F}_i$ presents the resultant force acting on the particle i. It may comprise the prescribed and contact forces. Rotational motion, if necessary, may be described in the same manner.

Methodology of calculating the contact forces in Eq. (1) depends on particle geometry and mechanical properties as well as on the constitutive model of particle interaction. The detailed

description of models employed in this work will be presented below. The integration of differential equations (1) for particle i at the time $t+\Delta t$ (where Δt is the time step) is performed numerically by applying the 5th order Gear's predictor-corrector scheme [4, 6, 28].

Normal contact

The mechanical behaviour of adhesive particles is essentially different from non-cohesive granular material. The presence of the load attraction force providing aggregation of dry adhesive particles is their characteristic feature.

A concept of the impact of adhesive particles is described by considering nonlinear elastic-plastic-dissipative contact behaviour. The focus of the investigation is to model smooth, isotropic and stiff spherical particles that are approaching soft contacts. Thus, contact displacement (overlap size) h is assumed to be small compared to the size (diameter) d of the stiff particle.

The evaluation of interparticle forces is based on the evaluation of a separate force F_{ij} acting between the particles i and j. Hence, the interaction force F_{ij} found between two particles i and j is expressed only in terms of the normal component $F_{ij} \equiv F_{ij}^n$.

A constitutive model comprising force-displacement relations in the form of algebraic functions has to be elucidated for these purposes. Typically, a load-displacement diagram is plotted in the nanoscale. It has the first loading path and a series of hysteretic loops. A hysteretic path comprises a series of unloading-reloading cycles. The applicability of this model is based on a quasi-static assumption implying that a relative impact rate is much lower than the speed of sound in the material. This allows us to treat the collision process as a sequence of equilibrium states.

Conceptually, normal contact may be described by considering a classical visco-elastic "spring-dashpot" model [3] supplied by adhesion (Fig. 1a). The spring model is assumed to be history independent and the accumulation effect is not considered. In this case, pressure and compression are defined as positive, while tension and extension are assumed to be negative.

Consequently, the normal interaction force occurring in binary collision of particles comprises three components of slightly different nature as follows:

$$F_{ij}^n = F_{spring}^n + F_{adh}^n + F_{diss}^n , \qquad (2)$$

where F_{spring}^n is contact deformation, or spring force, F_{adh}^n is adhesion force and F_{diss}^n is dissipation, or dashpot force. Various linear and non-linear models may be applied to evaluate particle contact force components.

A realistic and theoretically motivated nonlinear contact is governed by the Hertz contact theory for smooth spheres.

According to it, the elastic repulsion force $F_{spring}^n = F_{el}^n$ of the contacting particles depends on the overlap height h, while the power law defined by factor $\alpha = 3/2$ can be expressed as

$$F_{el}^n = K_{el}^n h^{\alpha} . \qquad (3)$$

Here, the nonlinear stiffness constant is:

$$K_{el}^n = \frac{4}{3} E_{ij}^{eff} \left(R_{ij}^{eff} \right)^{2-\alpha} , \qquad (4)$$

where

$$E_{ij}^{eff} = \frac{E_i E_j}{E_i\left(1-\nu_i^2\right)+E_j\left(1-\nu_j^2\right)}\ ; \qquad R_{ij}^{eff} = \frac{R_i R_j}{R_i + R_j}\ . \tag{5}$$

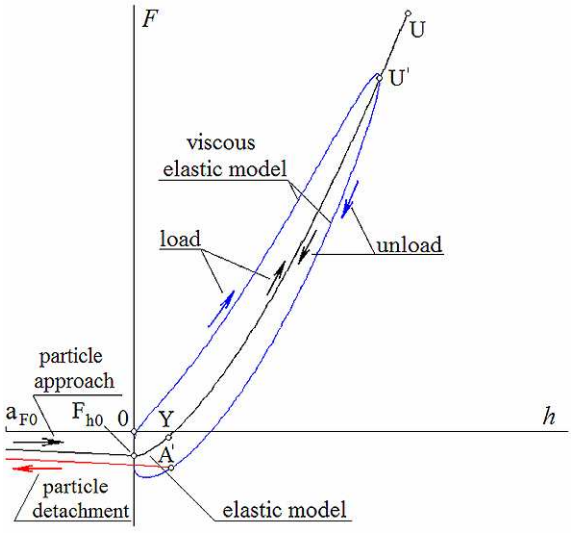

a)

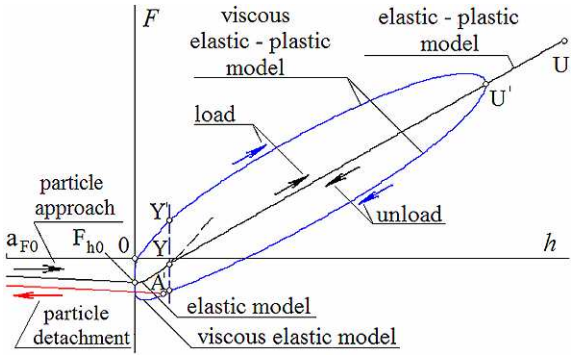

b)

Fig. 1. Models for normal contact of smooth adhesive spherical particles: a) elastic and visco-elastic model, b) elastic-plastic-viscous model with adhesion

Eq. (5) describes the effective contact elasticity modulus and the effective radius of particles *i* and *j*, respectively, where E_i and E_j are elasticity moduli and ν_i and ν_j are Poisson's ratios of particles *i* and *j*. Unloading, beginning at arbitrary point *U'*, is assumed to recover deformation path defined by Eqs. (3-5). In the presence of an arbitrary dissipation mechanism, unloading-reloading will follow a different path *U'-A*.

In order to reflect energy dissipation, the normal force may directly contain the viscous dissipation term $\boldsymbol{F}_{diss}^{n}$, as shown in Eq. (2). A review and systematic analysis of the known and the new extended models for normal contact and their comparison to the available experimental data are presented by Kruggel-Emden et al. [29]. In this work, different dissipation mechanisms and their applicability are discussed. However, they are restricted to non-cohesive interaction.

Generally, dissipation is based on analogy with that hold in the Hertz theory. Thus, non-liner damping force reads as follows:

$$F_{diss}^{n} = C_{diss}^{n}\dot{h}\,. \qquad (6)$$

Various approaches are used to evaluate the nonlinear characteristic C_{diss}^{n}, which is the displacement - dependent damping coefficient and $\dot{h}$ is the displacement rate. Kuwabara and Kono [30] intuitively proposed a fully nonlinear model combining spring and dissipative forces. This model was also independently derived by Brilliantov et al. [25]. Tsuji et al. [31] proposed a Hertz-type force law including a slightly modified dissipative term with a different exponent. Finally, non-linear dissipative constant C_{diss}^{n} was expressed in terms of the reduced mass and stiffness (5)

$$C_{diss}^{n} = \alpha_d \sqrt{m_{ij}^{eff} K_{spring}^{n}}\, h^{1/4}, \qquad (7)$$

where α_d is adjustable non-dimensional damping coefficient.

An adhesive contact starts when the surface distance between particles is in a range a few nanometers $|h| \le |a_{F0}|$, which means the short-range adhesion force without any contact deformation (the so-called jump in). This model presents the simplest case of a realistic van der Waals force.

Particles *i* and *j* still attract each other if the gap $|h|$ between their surfaces is smaller than the separation range $|a_{F0}|$, or $a_{F0} \le h \le 0$

$$F_{adh}^{n} = \frac{F_{h0} a_{F0}^{2}}{\left(a_{F0} + h\right)^{2}}\,. \qquad (8)$$

The particle approach curve in Fig. 1 contains two essential parameters: maximum attractive force $|F_{h0}|$ at minimum separation range $|a_{F0}|$.

As follows from Fig. 1a, at detachment point *A'* with overlap h_A, the contact unloading curve reaches the adhesion limit curve:

$$F(h_A) = -\pi R_{ij}^{eff}\, p_f \kappa_p h_A + F_{h0}\,. \qquad (9)$$

Expression (9) describes line *Y-U* and reflects the plastically deformed circular contact zone [26, 27]. Particles' detachment by contact expansion or negative surface separation *h* is expressed as:

$$F_{adh}^{n} = -\frac{\pi R_{ij}^{eff}\, p_f \kappa_p h_A}{\left(\left|a_{F0} + h - h_A\right|\right)^{3}} |a_{F0}|^{3} + \frac{F_{h0} a_{F0}^{2}}{\left(a_{F0} + h - h_A\right)^{2}}\,. \qquad (10)$$

Here, the second term expresses the influence of the accumulated plastic deformation during contact. The dimensionless plastic repulsion coefficient κ_p describes a dimensionless ratio of the attractive van der Waals pressure of a plate-plate model to the constant repulsive micro-yield strength p_f (hardness).

The model for the normal contact under consideration is based on the recent developments by Tomas [26, 27]. It combines nonlinear elastic – plastic contact behaviour and load-dependent non-linear model of adhesion. The new features of this model are described below in this paper.

From Fig. 1b it is obvious that the contact area may be initially loaded from point F_{h0} to *Y*, and, in response, is elastically deformed with an approximated circular contact area. At the elastic stage, nonlinear contact behaviour is governed by Hertzian model Eqs. (3-4). With increasing external normal load, the soft contact starts at the pressure p_f, with plastic yielding at the point *Y*. The particles' overlap h_Y at the point *Y* can be calculated by the Tomas [26, 27] formula:

$$h_Y = R_{ij}^{eff}\left[\frac{3\pi p_f\left(\kappa_A - \kappa_p\right)}{2E_{ij}^{eff}}\right]^2, \qquad (11)$$

where, κ_A is the dimensionless elastic – plastic contact area coefficient representing the ratio of plastic particle contact deformation area to the total contact deformation area.

As a consequence, the spring force in loading is defined by a generalized expression:

$$F_{spring}^n = \beta_{el}F_{el}^n + \beta_{el-pl}F_{el-pl}^n. \qquad (12)$$

Contact coefficients β_{el} and β_{el-pl} depend on contact specification. When the contact is elastic, $\beta_{el}=1$ and $\beta_{el-pl}=0$, while when the contact is elastic – plastic, the coefficients' values are $\beta_{el}=0$ and $\beta_{el-pl}=1$. Finally, the elastic – plastic contact force reads as:

$$F_{el-pl}^n = \pi R_{ij}^{eff} p_f\left(\kappa_A - \kappa_p\right)h. \qquad (13)$$

It is obvious that the yield limit cannot be exceeded; however, at a certain point *U*, unloading can begin. The nonlinear spring stiffness is extracted from Eqs. (3, 12-13). Constitutive equations (2-13) serve as the basis for simulation of impact.

Numerical investigation of normal contact

Normal contact at the impact of two identical spherical particles is considered numerically. The numerical experiment assumes that a mobile particle impacts the fixed target particle. Contact behaviour is considered by integrating the equations of motion (1) and applying various combinations of elastic-plastic-dissipative contact models with adhesion Eqs. (3-13). The numerical experiment conducted with particles defined by constant radius R_{ij}^{eff} = 0.3 μm is illustrated in Fig. 2. The mobile particle is induced by a portion of kinetic energy which is controlled by the initial impact velocity υ_0. Impact velocity serves as the basis for the initial conditions.

During the impact characterized by the loading path F_{h0}-*U'* (Fig. 1b), the particles collide and undergo elastic and (later) elastic-plastic deformation, while the induced kinetic energy is transformed to elastic deformation energy and partially dissipated. At a certain time instant, the mobile particle reaches the state of rest characterized by zero velocity $\upsilon = 0$ and the maximum overlap $h = h_{\max}$. After reaching the maximum overlap, the mobile particle starts to separate and follows the unloading path *U'*-*A'*.

The behaviour of adhesive particles during unloading largely depends on the imposed energy. If energy is high, at a certain time instant, the elastic and dissipative forces exceed the

adhesive limit $\left|F^n\right| > \left|F^n_{adh\_lim}\right|$, and the particles begin to detach (Fig. 2c). For lower impact rates a different scenario can be observed. If the imposed energy is insufficient to exceed the adhesive potential, the particles remain stuck together (Fig. 2d) and compression-tension oscillates, while kinetic energy is dissipated by viscous deformations until the equilibrium is reached.

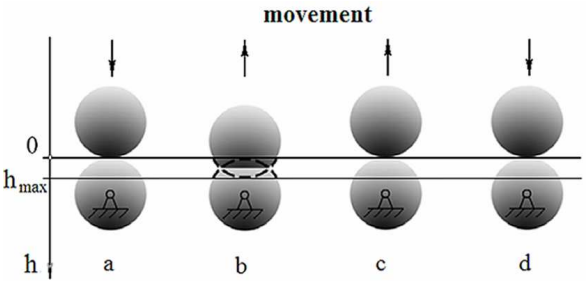

Fig. 2. The behaviour of particle during impact: a) loading b) unloading , c) detachment, d) sticking

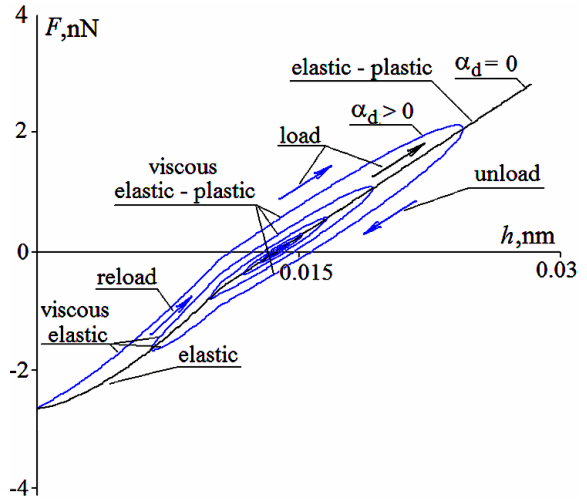

Fig. 3. A view of particles during normal impact: sticking behaviour with oscillations, when $\alpha_d = 0.2$

The microscopic adhesion parameters of adhesive particles are with the mechanical properties of limestone [26, 27]: adhesion force of the sphere-sphere contact F_{h0} = -2.64 nN, micro yield strength p_f = 300 MPa, plastic repulsion coefficient κ_p = 0.153, and elastic-plastic contact area coefficient κ_A = 5/6. Five values of the damping factor $\alpha_{d1} = 0$; $\alpha_{d2} = 0.2$; $\alpha_{d3} = 0.3$; $\alpha_{d4} = 0.4$; $\alpha_{d5} = 0.5$ of the Tsuji model [31] were explored in simulations. The values of damping factor applied were chosen in order to reflect the identical coefficients of restitution due to viscous dissipation. The above values of damping factors respond to coefficients of restitution: $\xi_1 = 1.0$; $\xi_2 \approx 0.76$; $\xi_3 \approx 0.65$; $\xi_4 \approx 0.56$; $\xi_5 \approx 0.48$. The case of zero damping $\alpha_d = 0$ illustrates non-viscous elastic-plastic adhesive behaviour, Fig 3.

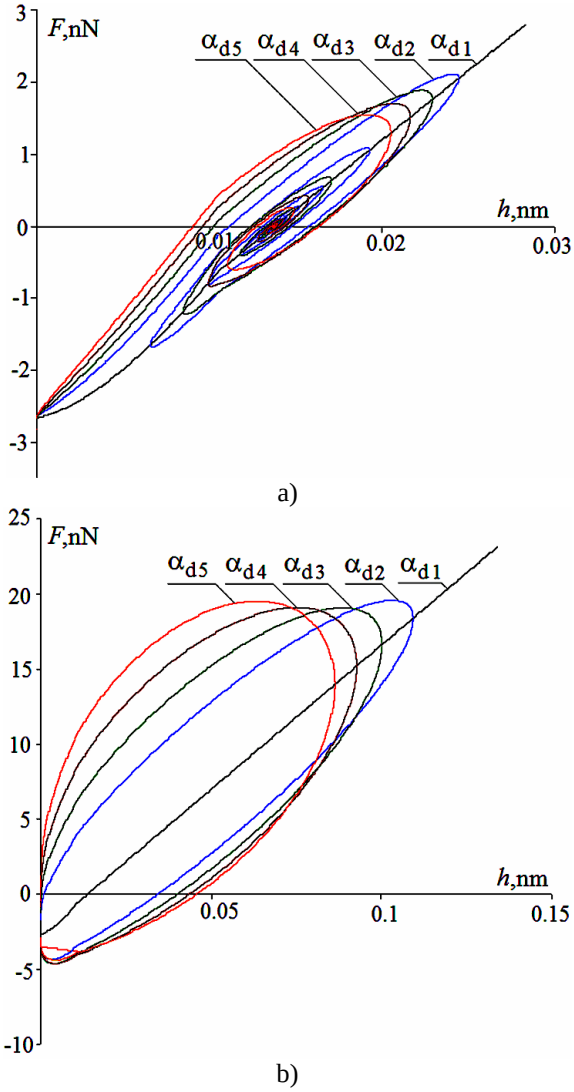

Fig. 4. Contact behaviour of particles during normal impact: a) υ_0 = 2 mm/min; b) υ_0 = 2 m/min damping factor α_{d2} = 0.2; α_{d3} = 0.3; α_{d4} = 0.4; α_{d5} = 0.5

The influence of impact energy was investigated by considering two values of impact velocity: υ_{01} = 2 mm/min and υ_{02} = 2 m/min. Contact behaviour in terms of load-displacement relationship for various damping ratios is shown in Fig. 4. Here, normal force comprises all inter-particle (right hand) forces, including viscous dissipation.

The higher impact velocity is of restitutive character and results in detachment of particles occurring after the single loading–unloading loop (Fig. 4a). On the contrary, low velocity is of adhesive character and leads to sticking and highly hysteretic oscillations (Fig.4b).

The present approach deals with numerical DEM simulations supported by sensitivity analysis. Two types of contact models for the range of effective particle radius R_{ij}^{eff}, varying between 0.1 and 1 μm for both elastic and elastic-plastic models combined with dissipative Tsuji damping model Eqs. (6-7), were examined.

The elastic loading path was defined by Eqs. (3-5), while elastic-plastic loading path was determined by Eqs. (13). The variation of the critical sticking velocity as a function of particle radii in logarithmic scale is illustrated in Fig. 5.

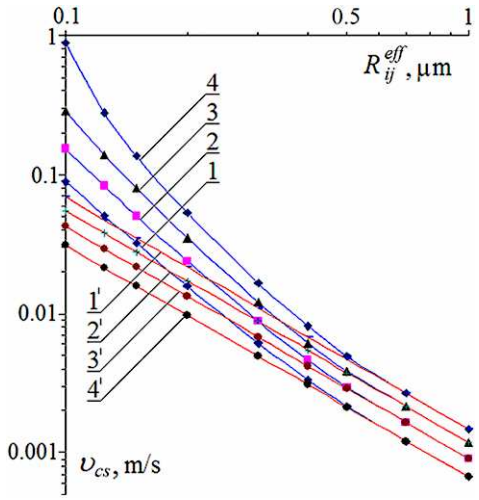

Fig. 5. Variation of critical sticking velocity versus effective radius for different loading models, with the damping factor values $\alpha_{d2} = 0.2$; $\alpha_{d3} = 0.3$; $\alpha_{d4} = 0.4$; $\alpha_{d5} = 0.5$

Here, the straight lines 1', 2', 3' and 4' exhibit the results obtained in using the elastic model, while curves 1, 2, 3 and 4 illustrate the increased role of elastic-plastic deformation for smaller particles. Line numbers indicate the values of damping factor $\alpha_{d2} = 0.2$; $\alpha_{d3} = 0.3$; $\alpha_{d4} = 0.4$; $\alpha_{d5} = 0.5$. The character of the graphs complies with the tendency reported in [25].

Concluding remarks

A characteristic feature of normal collision of adhesive particles exhibiting adhesive and restitutive behaviour was studied numerically by applying DEM. The influence of adhesion was studied for a wide range of effective particle radii, varying between 0.1 and 1 μm. This influence is illustrated by the variation of critical sticking velocity for both elastic and elastic-plastic models

On the basis of the numerical results, obtained in the investigation, some conclusions could be drawn. Generally, adhesion significantly affects agglomeration of smaller particles. Critical sticking velocity υ_{cs} decreases if the effective radius of the particle is higher. The same applies to the millimeter range particles, where critical sticking velocity and adhesion effects have no sense. The propagation of plastic deformation observed in the soft contact model increases critical sticking velocity, considerably deviating from the elastic solution when the particle size is decreased. The increase of viscous damping considerably increases this tendency. The assumptions on non-linear adhesion simplifying the spring model neglect, however, the additional dissipation mechanisms. Therefore, further research is required.

Acknowledgements

This work originated during the visit of the first author to Magdeburg supported by the German Academic Exchange Service under Grant ref. No. 323, PKZ/A 0692650.

References

[1] Jaeger H. M., Nagel S. R., Behringer R. P. Granular solids, liquids, and gases. Reviews of Modern Physics 68 (4), p. 1259-1273, 1996.

[2] Herrmann H. J. Granular matter, Physica A 313. p. 188 – 210, 2002.

[3] Cundall P. A. and Strack O. D. L. A discrete numerical model for granular assemblies. Geotechnique, 29(1), p. 47-65, 1979.

[4] Allen M. P. and Tildesley. D. J. Computer simulation of liquids. Oxford Science Publication, 1987.

[5] Herrmann H. J. and Luding S. Modelling granular media on the computer. Continuum Mech. Thermodyn, 10, p. 189-231, 1998.

[6] Džiugys A. and Peters B. J. An Approach to Simulate the Motion of Spherical and Non-Spherical Fuel Particles in Combustion Chambers. Granular Material, 3(4), p. 231-266, 2001.

[7] Pöschel T. and Schwager T. Computational granular dynamics, Models and algorithms. Springer, Berlin, 2004.

[8] Balevičius R., Džiugys A., Kačianauskas R. Discrete element method and its application to the analysis of penetration into granular media, Journal of Civil Engineering and Management 10 (1) p. 3-14, 2004.

[9] Balevičius R., Džiugys A., Kačianauskas R., Maknickas A., Vislavičius K. Investigation of performance of programming approaches and languages used for numerical simulation of granular material by the discrete element method. Computer Physics Communications 175, p. 404-415, 2006.

[10] Maknickas A., Kačeniauskas A. Kačianauskas R., Balevičius R., Džiugys A. Parallel DEM Software for Simulation of Granular Media. Informatica, 17(2), p. 207-224, 2006.

[11] Balevičius, R., Markauskas, D. Numerical stress analysis of granular material. – Mechanika, v. 4, No 66, p. 12-17, 2007.

[**12] Johnson K. L., Kendall K., Roberts A. D.** Surface energy and the contact of elastic solids. Proc. R. Soc. Lond. A, p. 301-313, 1971.

[13] Derjuguin B. V., Muller V. M., Toporov Y. P. Effect of contact deformations on the adhesion of particles. Journal of Colloid and Interface Science, 53(2), p. 314- 325, 1975.

[14] Molerus O. Theory of yield of cohesive powders. Powder Technol., 12, p. 259-275, 1975.

[15] Molerus O. Effect of interparticle cohesive forces on the ow behaviour of powders. Powder Technol., 20, 161-175, 1978.

[16] Thornton C. and Yin K. K. Impact of elastic spheres with and without adhesion. Powder Technol., 65, p. 153-166, 1991.

[17] Kohring G.A. Computer simulations of granular materials: the effects of miesoscopic forces. Phys. I France, 4, 1779-1782, 1994.

[18] Tomas J. Assessment of mechanical properties of cohesive particulate solids: Part 1. Particle contact constitutive model. Part. Sci. Technol., 19, 95- 110, 2001.

[19] Tomas J. Assessment of mechanical properties of cohesive particulate solids:Part 2. Powder flow criteria, Part. Sci. Technol., 19, p. 111- 129, 2001.

[20] Tomas J. Fundamentals of cohesive powder consolidation and flow. Granular Matter 6, p. 75-86, 2004.

[21] Luding S., Tykhoniuk R., Tomas J. Anisotropic material behaviour in dense, cohesive powders. Chem. Eng. Technol., 26(12), p. 1229- 1232, 2003.

[22] Luding S. Shear flow modeling of cohesive and frictional fine powder. Powder Technology, 158(1-3), 45-50, 2005.

[23] Tykhoniuk, R., Tomas, J., Luding, S., Kappl, M., Heim, L. and H.-J. Butt, Ultrafine cohesive powders: from interparticle contacts to continuum behaviour, Chem. Engng. Sci. 62, p. 2843-2865, 2007

[24] Gilabert F. A., Roux J.-N., Castellanos A. Computer simulation of model cohesive powders: Influence of assembling procedure and contact laws on low consolidation states. Physical review E, 75, 011303, p. 1-25, 2007.

[25] Brilliantov V. N., Albers N., Spahn F., Poschel T. Collision dynamics of granular particles with adhesion. Physical Review E, 76, 051302, 2007.

[26] Tomas J. Adhesion of ultrafine particles. A micromechanical approach. Chemical Engineering Science, 62, p. 1997- 2010, 2007.

[27] Tomas J. Adhesion of ultrafine particles. Energy absorption at contact. Chemical Engineering Science, 62, p. 5925- 5939, 2007.

[28] Jasevičius R., Kačianauskas R. Modelling deformable boundary by spherical particle for normal contact. Mechanika, 6(68). p. 513, 2007.

[29] Kruggel-Emden H., Simsek E., Rickelt S., Wirtz S., Scherer V. Review and extension of normal force models for the Discrete Element Method. Powder Technol., 171(3), p. 157-173, 2007.

[30] Kuwabara G., Kono K. Restitution coefficient in a collision between two spheres. Japanese Journal of Applied Physics, 26, p. 1230-1233, 1987.

[31] Tsuji Y., Tanaka T., Ishida T. Lagrangian numerical simula
tion of plug of cohesionless particles in a horizontal pipe.
Powder Technol., 71, p.239-250, 1992.